Autowave process of the localized plastic deformation of high-chromium steel saturated with hydrogen

A V Bochkareva[1,2], S A Barannikova[1,3,4], Yu V Li[1], A G Lunev[1,2] and L B Zuev[1,3]

[1] Institute of Strength Physics and Materials Science, SB RAS, Tomsk, 634055, Russia
[2] National Research Tomsk Polytechnic University, Tomsk, 634050, Russia
[3] National Research Tomsk State University, Tomsk, 634050, Russia
[4] Tomsk State University of Architecture and Building, Tomsk, 634003, Russia

E-mail: avb@ispms.tsc.ru

Abstract. The deformation behavior of high-chromium stainless steel of sorbitic structure upon high-temperature tempering and of electrically saturated with hydrogen in the electrochemical cell during 12 hours is investigated. The stress-strain curves for each state were obtained. From the stress-strain curves, one can conclude that hydrogen markedly reduces the elongation to the fracture of specimen. Using double-exposed speckle photography method it was found that the plastic flow of the material is of a localized character. The pattern distribution of localized plastic flow domains at the linear hardening stage was investigated. Comparative study of autowave parameters was carried out for the tempered steel as well as the electrically saturated with hydrogen steel.

1. Introduction

In recent years, we have found experimentally for a range of metals and alloys that plastic deformation at all its stages is prone to localization [1,2]. The localization patterns observed are wave-like in character; the kind of wave depends on the acting law of work hardening, that is, the form of function $\theta(\varepsilon)$ [3]. There are only four of them: single deformation fronts move in the easy glide stage for single crystals and in a yield plateau for polycrystals; a system of equidistant mobile localized-strain centers in the linear hardening stage; spacio-periodic structure of plastic strain localization regions in the Taylor parabolic work hardening stage, and the structure of nonuniform mobile strain-localization regions peculiar to the final (prefracture) deformation stage.

These surveys of the localized-strain pattern features for the high-chromium stainless steel widely used in water-vapor, aquatic and acid environments, provide means of getting more information about material behavior being part of a critical structure. For example, a chemical reactor or oil and gas equipment made of high-chromium stainless steel operate in the presence of sever atmosphere of hydrogen. The presence of hydrogen (H) in solid solution of metals and alloys is related mainly to the small diameter of this element and its capacity to diffuse with certain ease in solid state. Different factors contribute to elevate or diminish the solubilization and/or diffusion of H in steels. The main ones are temperature, alloy composition, crystalline structure and substructure. Nevertheless, the presence of H in metals, particularly in steels, is not desired in most of the cases, since H alters considerably the mechanical–metallurgic properties of these materials with the possibility of fracture [4-8]. The main aim of this investigation was to elucidate the effect of dissolved hydrogen on the macroscopic plastic flow localization patterns in tensile strained stainless steel polycrystals.

2. Test material and investigation technique

The investigation was performed using specimens of high-chromium stainless steel (0.4%C–0.6%Si–0.55%Mn–12.5%Cr). The specimens were configured as dog bones with the gage section measuring 50×10×2 mm. The test pieces were cut out from sheet steel along the rolling direction. According to condition of supply, this steel has a ferrite-carbide structure; therefore, it was subjected to heat treatment [9, 11]. The specimens were quenched at T = 1320 K for 3 hours by fast air cooling to provide a martensitic high-strength structure with a small amount of chromium carbides. After that, in order to increase plasticity, the specimens were under high-temperature tempering from T = 870 K for 3 hours and furnace cooling, so that sorbitic structure (ferrite and carbides) was generated (figure 1).

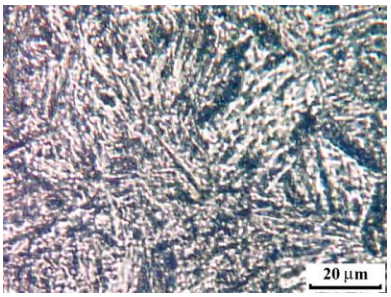

Figure 1. Microstructure of high-chromium steel in tempered state.

Prepared in this manner, the specimens were electrically saturated with hydrogen. The electrolytic hydrogenation of alloy samples was carried on for 12 and 24 hours under a controlled cathode potential of –600 mV relative to a reference electrode of silver chloride in the 0.1N solution of sulphuric acid with addition of 20 mg/L of thiourea [10]. The current-voltage curves were recorded using an IPC-Compact potentiostat. The time between hydrogen charging and tensile testing did not exceed 30 min and the testing time was less than 60 min. The specimens were subjected to uniaxial tension at room temperature at the rate of $6.67 \cdot 10^{-5} s^{-1}$ using a universal testing machine LFM-125 (Switzerland). The stress-strain curves for the material are shown in figure 2. The plastic flow curves plotted for the samples tested in tension were analyzed to single out a linear-hardening flow stage, whereas work hardening coefficient $\theta = const$. Concurrently, the displacement vector fields of points on the surface of the specimens were recorded by a double-exposure speckle detailed in [3]. An analysis of the spatial-periodical distribution of local elongation ε_{xx} of the specimen observed in the linear-hardening stage makes it possible to estimate the autowave spacing λ as well as velocity $V_{aw} = dX / dt$.

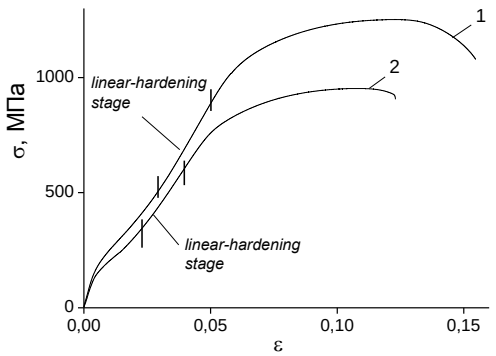

Figure 2. Stress-strain curves for high-chromium steel in the tempered state (1) and after electrolytic hydrogenation for 12 h (2).

The deformation diagrams for the alloy under review refer to the general type diagrams, therefore can be described by the Lüdwick equation [12]

$$s = s_0 + \theta e^n \tag{1}$$

where s is the true stress and can be calculated as $s = \sigma(1+\varepsilon)$, e is the true strain calculated as $e = \ln(1+\varepsilon)$, $s_0 \approx \sigma_y$ is the true critical share stress, $\theta = d\sigma/d\varepsilon$ is the work hardening coefficient expressed in MPa units, as it is a stress, and $n \le 1$ is the work hardening exponent.
In different portion of the stress-strain curve constructed in $\ln(s - s_0) - \ln e$ coordinates, the strain exponent has different values, but for the certain deformation stage, there are particular constant values of n and θ. For the linear work-hardening stage, n should be equal to 1.

3. Linear work-hardening stage and autowaves of plasticity

Hydrogen charging for 12 hours (2) results in remarkable changes of stress-strain curves as shown in figure 2. It is found that a 35 % decrease in the yield stress and 26 % decrease in the ultimate stress are observed for the counterpart subjected to hydrogenation for 12 hours (2) relative to the tempered samples of steel (1). From the obtained stress-strain curves, one can conclude that hydrogen markedly reduces the elongation to the fracture of specimen. The results obtained for the high-chromium steel electrically saturated with hydrogen for 24 hours [13] show the further decrease in mechanical properties of the material tested. It is found a 70 % decrease in the yield stress and 40 % decrease in the ultimate stress relative to the tempered samples of steel. The mechanical properties of the studied steel in different states are summarized in table 1.

One can see from the table 1 that the stress-strain curves of steel in all three states were found to include the linear work-hardening stage.

Table 1. Mechanical properties of stainless steel in different states.

	σ_y, MPa	σ_B, MPa	δ, %	θ, GPa	Linear work-hardening stage, n≈1	
					ε_{in}	ε_{tot}
Tempered	218	1251	12.9	19.3	0.03	0.054
12 h hydrogenation	141	922	9.9	14.7	0.024	0.037
24 h hydrogenation	73	798	4.7	14.6	0.047	0.058

The plastic-strain localization patterns for each of the stress-strain curves were studied by the double-exposure speckle photography. The displacement-field data for strained specimens were transformed into spatial distributions of local elongations ε_{xx}, using numerical differentiation as it shown in figure 3 for the tempered stainless steel.

So, if the distribution is spatial, the spatial period (λ) can be determined (figures 3 and 4). It should be noted that the spatial period of local elongation distribution significantly decreased after electrolytic hydrogenation of tempered steel specimen in the three electrode electrochemical cell. As a result, the localized-strain centers became clearly visible, and the coordinate of localized maximum can be determined.

As the local distributions of elongation component ε_{xx} in the linear-hardening stage in the tempered steel and in the steel saturated with hydrogen are of the periodic spatio-temporal structure and one have the sequence of these distributions in time, the positions of the strain centers as a function of the loading time can be plotted, as it shown in figure 5 for the high-chromium steel in the studied states. The sequence of coordinates for each of the localized plastic deformation domains in this stage is

approximated by nearly parallel straight lines, where the slope of the curves enables the velocity of the domains to be estimated $V_{aw} = dX / dt$.

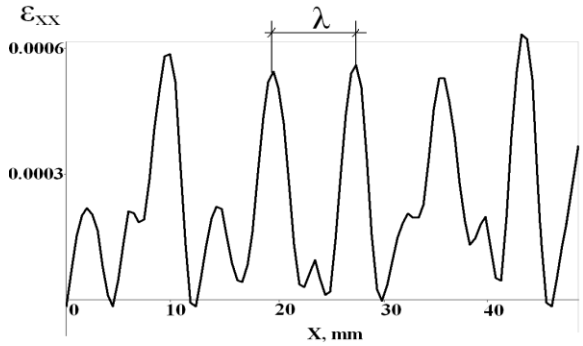

Figure 3. Distribution of local elongation component over tension axial: tempered steel in the linear-hardening stage

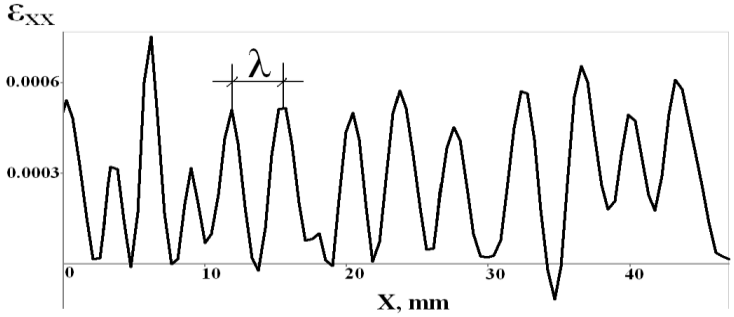

Figure 4. Distribution of local elongation component over tension axial: tempered steel saturated with hydrogen (12h) in the linear-hardening stage

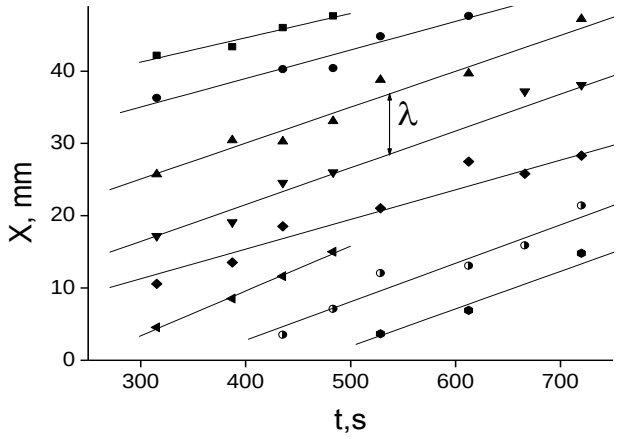

Figure 5. Mobile localized centres of local elongation component for the tempered high-chromium stainless steel.

Figure 4 shows the spatial distributions of local elongations ε_{xx}, for the steel saturated with hydrogen for 12 hours. Thus, all strain centers are seen to move uniformly at nearly the same velocities to generate the phase autowave [3, 13]. The autowave velocity V_{aw} was determined from the slopes of the

X(t) curves, whereas the autowave length (λ) was found from the curve spacing measured along the axis X. For the tempered specimen, the autowave length and autowave velocity are λ=6.8±1.5 mm and V_{aw}=(4.9±0.9)×10^{-5} m/s, correspondingly. As for the steel specimen after electrolytic hydrogenation, λ=4.6±0.5 mm and V_{aw}=(4.0±0.7)×10^{-5} m/s. The autowave velocity and length for the states studied are given in Table 2.

Table 2. The characteristics of localized-strain autowaves.

	λ, mm	$V_{aw}\times10^5$ m/s
Tempered	6.8±1.5	4.9±0.8
12 h hydrogenation	4.6±0.5	4.0±0.7
24 h hydrogenation	3.5±0.5	3.9±0.8

The comparing analysis of spatial distribution of local elongation for the specimen observed in the linear-hardening stage for the tempered state was conducted using the standard statistical processing data obtained such Student's t-criteria [15]. According to this, experimental results should be intercompared by the equation

$$t = (\bar{x}_1 - \bar{x}_2)\cdot\left(\frac{(n_1-1)\cdot s_1^2 + (n_2-1)\cdot s_2^2}{n_1+n_2-2}\right)^{-\frac{1}{2}}\cdot\left(\frac{n_1\cdot n_2}{n_1+n_2}\right)^{\frac{1}{2}} \quad (2)$$

where $\bar{x}_1, \bar{x}_2$ are the average values of two sampled populations, n_1, n_2 – the units in the sample, s_1, s_2 – the dispersion.

Using Student's t-criteria for the certain confidence level $\alpha = 0.95$, one must compare $|t|$ calculated with the tabulated value of $t_{\alpha,f}$. If the calculated value exceeds the tabulated one, it means that two average values differ significantly.

The resultant quantity $|t| \geq t_{\alpha,f}$ is true for the value of the autowave length λ. This fact suggests that the average λ-values obtained for the tempered alloy and the hydrogenated one are quite different from each other. For the autowave velocity V_{aw} the $|t| \geq t_{\alpha,f}$ expression is not justified, so one can say that the velocity of autowave propagation is almost not change.

It is found experimentally that the motion rate of localization nuclei observed at the stage of linear work hardening is inversely proportional to the work hardening coefficient. This dependence is common to all the metals and alloys investigated [3, 16]. The shape of this dependence ($V_{aw} \sim 1/\theta$) indicates that the wave processes in question differ in nature from the well-known plasticity waves (Kolsky waves) for which the dependence has the following form $V_{pl} \sim \sqrt{\theta}$ (here ρ is density). The distinction between the above two dependences leads one to conclude that a new type of wave processes is discovered. They are self-excited waves of the plastic flow. The new type waves will be generated in the deforming specimen, irrespectively, of electrolytic hydrogenation [10, 13, 14].

4. Conclusion

The deformation behavior of high-chromium stainless steel subjected to high-temperature tempering and saturated with hydrogen in three electrode electrochemical cell at controlled constant cathode potential for 12 and 24 hours was investigated. The mechanical properties of the steel in three states were detected. The hydrogen charging for 12 hours results in remarkable changes of yield stress, ultimate stress and total elongation of material under study. The stress-strain curves of the examined states of the stainless steel are characterized by the linear work-hardening stage with constant values of $n \approx 1$ and θ. Because of this, phase autowave of plasticity occurs for steel in the states mentioned above.

Hydrogen not only provides the remarkable softening effect on the high-chromium stainless steel but it also initiates the significant reconstruction in the spatial scale for distribution and magnitude of plastic strain. The change in the microstructure of hydrogen charged tempered steel affects the stress-strain curves as well as the plastic strain localization patterns.

The comparison of the data for two conditions (tempered condition and after hydrogenation condition) of steel showed that the hydrogen significantly enhances localization and changes the quantitative parameters of the macroscopic plastic strain localization, particularly, the wave length of autowave plastic strain localization. The mechanism of hydrogen-stimulated plastic strain localization is still under discussion.

Acknowledgments
The work was performed in the frame of the Tomsk State University Academic D.I. Mendeleev Fund Program, of the Program of Fundamental Research of State Academies of Sciences for the period 2013-2020 yrs. and was partially supported by the Russian Foundation for Basic Research (Project No. 16-08-00385-a)

References

[1] Fressengeas C, Beaudoin A, Entemeyer D, Lebedkina T, Lebyodkin M and Taupin V 200 *Phys. Rev.* B **79** 014108
[2] Asharia A, Beaudoin A and Miller R 2008 *Math. Mech. Sol.* **13** 292–315
[3] Zuev L B and Barannikova S A 2014 *Int. J. Mech. Sci.* **88** 1–8
[4] Hudson R M and Stragand G L 1960 *Corros.* **16** 253–57
[5] Hirth J P 1980 *Met. Trans.* **11A** 861–90
[6] Fuchigami H, Minami H and Nagumo M, 2006 *Phil. Mag. Lett.* **86** 21–9
[7] Sofronis P, Liang Y and Aravas N 2001 *Eur. J. Mech. A Solid.* **20** 857–72
[8] Robertson I M 2001 Eng. *Frac. Mech.* **68** 671–92
[9] Pelleg J 2013 *Mechanical properties of materials* (New York, London: Springer–Dordrecht–Heidelberg) p 620
[10] Zuev L B, Barannikova S A , Nadezhkin M V and Mel'nichuk V A 2011 *Techn. Phys. Lett.* **37** 793–6
[11] Firger I V 1982 *Thermal treatment of allows. Reference book.* (Leningrad: Mashinostroyenie Publ.) p 304
[12] Trefilov V I, Moiseev V F, and E P Pechkovskii 1989 *Strain Hardening and Fracture of Polycrystalline Metals* (Kiev: Naukova Dumka)
[13] Bochkareva A V, Barannikova S A, Lunev A G, Li Yu V and Zuev L B 2015 *Proc. of Int. Conf. on Mechanical Engineering, Automation and Control Systems* (Tomsk: IEEE) pp 1–3
[14] Barannikova S A, Lunev AG, Nadezhkin M V and Zuev L B 2014 *Adv. Mater. Res.* **880** 42–7
[15] Hudson D J 1964 *Statistics* (Geneva: CERN)
[16] Barannikova S A 2004 *Tech. Phys. Lett.* **30** 338–40